Chapter 1

Introduction

1.1 Fluid

Fluids are substances that are capable of flowing. Fluids can easily change their shape by rearranging their molecular structure. The main states of fluid that play a pioneering role in the earth and universe are liquid and gaseous. Moving and stationary fluids are required by nature. The movement of water in seas and rivers and the movement of air in the atmosphere are required for the existence of life in nature. Stationary fluids are also significant in our daily lives. The study of fluid's behaviour at rest (termed fluid statics) and in motion (termed fluid dynamics) is known as fluid mechanics. The major applications of fluid mechanics cover meteorology, transportation, food production, power generation, heat exchangers, nuclear reactors, biomedical equipment, air conditioning, aerospace, oil production, and hydraulics design. The important fluid flow characteristics are described as follows:

1.2 Types of fluid flow

- Steady and unsteady flows
- Laminar and turbulent flows
- Rotational and irrotational flows
- Compressible and incompressible flows
- One,two and three-dimensional flows

1.2.1 Steady and unsteady flows

Fluid properties such as pressure, velocity, and density remain constant in the steady case at any point in time. The situation can be mathematically expressed as follows:

$$\frac{dv}{dt} = 0, \ \frac{dp}{dt} = 0 \ , \ \frac{d\rho}{dt} = 0. \tag{1.2.1}$$

Where v is the velocity, p is the pressure, ρ is the density and t is the time.

1.2.2 Laminar and turbulent flows

Laminar flow refers to the parallel and regular movement of fluid layers sliding one over the other. Consider the motion of oil/water in a circular pipe that is slanted with an angle of inclination with the horizontal line. Laminar flow is observed in this case with fluid layers in the shape of concentric circular cylinders that move parallel to each other. Mixing of fluid layers or irregular fluid paths are not observed in this case. Further, fluid flow is stationary near the wall's surface and gradually increases near the pipe's center. In turbulent flow, irregular fluid paths and the mixing of fluid layers have occurred. Smoke movement near the cigarette is an example of laminar flow and the smoke movement becomes turbulent after a certain distance from the cigarette.

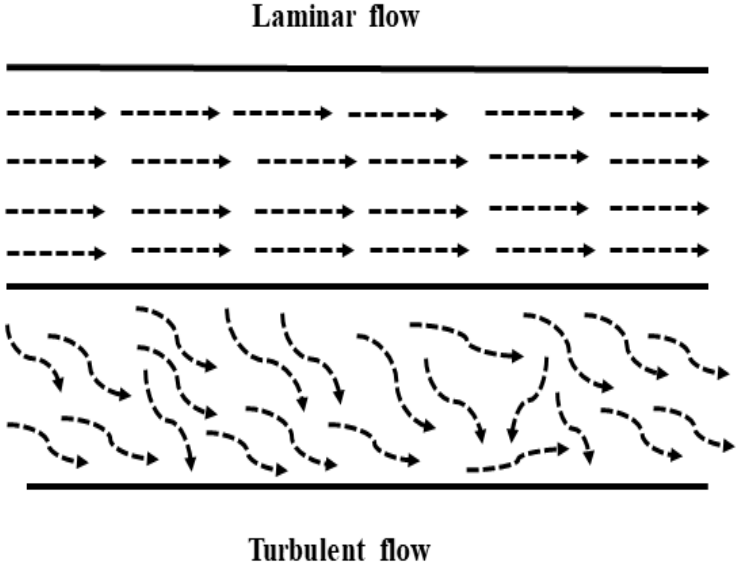

Figure 1.1: *Laminar and turbulent flows*

1.2.3 Rotational and irrotational flow

The movement of fluid particles about an axis is called rotational flow or swirling flow. $\Omega = \nabla \times V$ describes vorticity at any point of the fluid flow. Fluid particles in the flow field are rotating when $\Omega \neq 0$. Irrotational flow occurs when $\Omega = 0$.

1.2.4 Compressible and incompressible flows

Compressible fluids have a density that varies with pressure, whereas incompressible fluids have a constant density. Gases are more compressible than liquids. It is due to the larger space between gaseous molecules in the volume occupied by gases than liquids.

1.2.5 One, two and three-dimensional flows

Fluid flow can be classified as one, two, or three-dimensional depending on the number of space coordinates. The velocity, temperature, and concentration of the flow profiles in the one-dimensional form are explained with space and time coordinates whereas two-dimensional and three-dimensional flows are described with more than one space coordinate. Fluid flow past a stretching sheet with velocity varies in the x-direction forming a one-dimensional flow. In a two-dimensional flow, the velocity varies in both the x and y directions. If the velocity is a function of three space coordinates, say x, y, and z then a three-dimensional flow occurs.

1.3 Viscosity

Viscosity is an internal resistance (stress) in the movement of fluid particles. The fluid flow is degraded by viscosity. Oil, honey, and syrup have a high viscosity, whereas water, alcohol, and kerosene have a low viscosity. Viscous fluids exhibit tangential and normal stress with two contacting layers in motion. The reciprocal of viscosity is fluidity. Viscosity can be classified as follows:

- Dynamic viscosity
- Kinematic viscosity

Dynamic viscosity is the ratio of shear stress to shear rate that measures internal resistance to flow. Kinematic viscosity is defined as the ratio of dynamic viscosity to density.

1.4 Newtonian fluids

Newtonian fluids are fluids that exhibit unique viscosity with shear stress. Shear stress is a tangential force parallel to the cross-sectional area of a material. Alcohol, gasoline, and water are Newtonian fluids. These fluids obey Newton's law of viscosity and show a linear relationship between shear stress and shear rate. In other words shear stress formed by an external force is equal to the product of shear rate and fluid viscosity.

$$\tau_{yx} = \mu\dot{\gamma}_{yx} \tag{1.4.1}$$

In the relation, τ_{yx} is the shear stress due to a force on the cross-sectional area, $\dot{\gamma}_{yx}$ is the shear rate, and μ is the dynamic viscosity.

1.5 Non-Newtonian fluids

The fluid that doesn't follow Newton's law of viscosity is known as non-Newtonian fluid. Viscosity may increase or decrease depending on the shear rate and the type of fluid. Four types of non-Newtonian behavior are generally observed they are pseudoplastic, dilatant, thixotropic, and rheopectic respectively. They are further divided into time-dependent and time-independent fluids.

1.5.1 Pseudoplastic fluids

Pseudoplastic fluids show an inverse functional relationship between shear stress and viscosity. Pseudoplastic fluids are time-independent. Blood and ketchup are examples of pseudoplastic fluid. These fluids are also known as shear-thinning fluids.

1.5.2 Dilatant fluids

Dilatant fluids show high viscosity with shear stress. They are also known as shear thickening fluids. dilatant fluids are time-independent. Oobleck and quicksand are examples of dilatant fluids.

1.5.3 Thixotropic fluids

Thixotropic fluids show a negative response between shear stress and viscosity. Thixotropic fluids are time-dependent when compared with pseudoplastic fluids. The viscosity of a thixotropic fluid decreases with time at a constant shear rate. Cosmetics paint and glue are thixotropic fluids.

1.5.4 Rheopectic fluids

Rheopectic fluids show a positive response between shear stress and viscosity. Rheopectic fluids are time-dependent when compared with dilatant fluids. The Viscosity of rheopectic fluids increases with time at a constant shear rate. Cream and gypsum paste are rheopectic fluids.

1.6 Carreau fluid model

In 1972, (Carreau, 1972) introduced the following viscosity model.

$$\frac{\mu - \mu_\infty}{\mu_0 - \mu_\infty} = \left\{1 + (\Gamma\dot{\gamma}_{yx}\ )^2\ \right\}^{\frac{n-1}{2}} \tag{1.6.1}$$

where Γ is the relaxation time, $\dot{\gamma}_{yx}$ is the shear rate, n is the power law index, μ_0 and μ_∞ represent the viscosities at low and high shear rates, respectively. Shear thinning and thickening behaviour depends on n. The viscosity model with $n > 1$ show a shear thickening nature and $n < 1$ exhibits a shear thinning nature.

1.7 Reiner Rivlin fluid

Reiner and Rivlin proposed a relationship for an isotropic fluid between the stress tensor τ_{ij} and the rate of strain tensor e_{ij}. The following constitutive relation is used to model the rheological properties of the Reiner-Rivlin nanoliquid (see (Tabassum & Mustafa, 2018)).

$$\tau_{ij} = -p\delta_{ij} + \mu_f e_{ij} + \mu_c e_{ik} e_{kj}, (e_{jj} = 0). \tag{1.7.1}$$

Here, the rate of strain (deformation) tensor is denoted by $\mathrm{e_{ij}} = \frac{\partial u_i}{\partial x_j} + \frac{\partial u_j}{\partial x_i}$, Kronecker delta symbol is denoted by δ_{ij}, coefficient of viscosity is denoted by μ_f, cross-viscosity coefficient is denoted by μ_c and pressure is denoted by p. The influence of stress across velocity gradients leads to cross-viscosity, a property of the Reiner-Rivlin nanofluid considered in the study.

1.8 Heat transfer

Heat transfer occurs due to temperature differences between two regions. The transmission of heat energy from one place to another is known as heat transfer. The heat transfer mechanism improves the finishing quality of many industrial

products while reducing the risk of electronic equipment damage due to overheating. Conduction, convection, and radiation are the main modes of heat transfer.

1.8.1 Conduction

Conduction is the process of heat transfer from a hot body to a colder one that occurs through direct contact. This mode of heat transfer is usually observed in solids and liquids. The molecules in direct contact with hotter ones start vibrating and transfer the energy to nearby molecules. The molecular movement is not observed in the case while free electrons transmit energy so vacuum space does not promote conduction. Metals are good conductors than others. According to Fourier's law, the heat transfer equation is mathematically described as follows:

$$q = -k\frac{dT}{dx} \tag{1.8.1}$$

where k is the coefficient of thermal conductivity, q is the quantity of heat and $\frac{dT}{dx}$ is the temperature gradient. Here the negative sign indicates the direction of heat from higher to lower temperature.

1.8.2 Convection

The process of replacement of hotter fluid particles with the colder ones is known as convection. This process of heat transfer usually occurs in gasses and liquids by the bulk/random movement of molecules. Mainly it happens due to temperature gradient and the contact of adjacent fluid layers with a hot solid boundary. The convection phenomenon can be further classified according to the nature of the flow as free convection and forced convection. Free convection is due to buoyancy force by the density variation while forced convection is due to an external force. A fan, pump and suction devices are required for a forced convection. According to Newton's law, the heat transfer equation is mathematically described as follows:

$$q = hA\left(T_w - T_\infty\right). \tag{1.8.2}$$

where A, h, T_w and T_∞ are the heat transfer area, convection heat transfer coefficient, temperature of the surface, and reference temperature respectively.

1.8.3 Radiation

The process of heat transfer from a region to another region in the form of electromagnetic waves is known as radiation. This mode of heat transfer doesn't require any medium. Solar energy from the sun and heat energy released from the filament of a bulb are examples of radiation. The sun's energy reaches the earth without heating the space between them and a similar phenomenon is observed in the case of heat produced from the filament of a bulb.

1.9 Mass transfer

Mass transfer is the movement of mass from a higher concentration zone to a lower region. A difference in species concentration of two or more component mixtures initiates the mass transfer phenomenon. The mass transfer exists in the process of drying, adsorption, distillation, evaporation, absorption, etc. Mass transfer can be due to mass diffusion or convective mass transfer. Mass diffusion occurs due to concentration differences in adjacent fluid layers whereas a moving fluid between a boundary surface leads to convective mass transfer.

1.10 Chemical reaction

The process in which one or more reactants are converted into new products that reaction is known as a chemical reaction. It may be homogeneous or heterogeneous. if the reactants and products are in the same phase then the chemical reaction is homogeneous otherwise it is heterogeneous. In a chemical reaction either heat is absorbed or generated. Exothermic reactions evolve heat energy whereas endothermic reactions absorb heat energy. If the reaction rate is directly proportional to concentration then it is a first-order chemical reaction. Chemical reaction has an important role in the heat and mass transfer processes. Fluid flow with chemical reaction has applications in polymer production, food processing, manufacturing of ceramics, etc.

1.11 Magnetohydrodynamics (MHD)

Magnetohydrodynamics is an area that discusses the coupled nature of fluid motion and magnetic field. The magnetic field generates a current in a moving conductive fluid that creates an induced magnetic field. Both the electric current and induced

magnetic field produce a force namely Lorentz force on the moving fluid that can alter the velocity and magnetic effects of the fluid. MHD flows can be found in nature. The magnetic field is generated due to the motion of the inner liquid metal core of the earth is a shield that protects the earth from harmful radiation. Sunspots and solar flares are real-life examples of MHD flow. Fluid flows in the industrial process are greatly influenced by a magnetic field. Heated liquid metals are Stirred, pumped, and levitated by utilizing a magnetic field.

The concept of MHD flows originated from the pioneering work of Swedish Physicist Alfven (Alfvén, 1942). He was honored with the Nobel prize in physics in the year 1970. Maxwell's equations for electromagnetism and Navier Stoke's equation for fluid mechanics are the basic equations that describe the governing equations of hydromagnetic fluid flows. The Solar wind, mercury, plasmas, seawater, salt water, and electrolytes are some examples of hydromagnetic fluids. MHD flows are widely used in metallurgy, polymer industry, plasma jet, electromagnetic pump, and aeronautics. Maxwell equations are defined as follows

Gauss's law

$$\vec{\nabla}.\vec{E} = \frac{\rho_e}{\epsilon_0}. \tag{1.11.1}$$

Faraday's law of induction

$$\vec{\nabla} \times \vec{E} = -\frac{\partial \vec{B}}{\partial t}. \tag{1.11.2}$$

Ampere's law

$$\nabla \times \vec{B} = \mu_0 \vec{J} + \mu_0 \ \epsilon_0 \frac{\partial \vec{E}}{\partial t} \tag{1.11.3}$$

Lorentz force

Moving fluid particles with velocity $\vec{v}$ and charge q in the presence of an external magnetic field experiences a force known as Lorentz force.

$$\vec{F} = q \ \left(\vec{E} + \vec{v} \times \vec{B}\right). \tag{1.11.4}$$

Gauss's law for magnetism

$$\nabla.\vec{B} = 0, \vec{B} = \mu_0 \ \vec{H}. \tag{1.11.5}$$

where E is electric field intensity, ρ_e is electric charge density, ϵ_0 is the permittivity of free space, μ_0 is the permeability of free space, H is the magnetic field intensity, B is the magnetic flux density, σ is the electric conductivity and J is the electric current density.

1.12 Hall current

Electrically conducting fluid in the presence of a strong magnetic field induces a current known as Hall current which is normal to both electric and magnetic fields. It was observed by Edwin Herbert Hall in 1879 (Hall et al., 1879). Hall effect causes a drift in the movement of charged particles due to gyration. Fluid flow with hall current has a significant role in micromixing of physiological samples, Nuclear reactor cooling, meteorological studies, MHD power generators, etc.
Ohm's law with Hall current can be described as follows

$$J + \frac{\omega_e \tau_e}{B_0} \ (J \times B) = \sigma \ \left(\vec{E} + \mu_e \overrightarrow{v} \times \vec{B}\right). \tag{1.12.1}$$

where v is the velocity vector, B is the magnetic field, B_0 is the strength of the magnetic field, J is the electric current density, μ_e is the magnetic permeability, ω_e is the cyclotron frequency and τ_e is the electron collision time. $\omega_e \tau_e$ is the Hall parameter.

1.13 Soret effect (Thermophoresis)

Hot or high-energy level fluid particles migrate towards the cold/low energy level region. Physically this is due to the temperature gradient. This force is known as thermophoresis force which accelerates the heat transfer process. This phenomenon is observed in a suspended mixture of fluid particles.

1.14 Joule heating effect

The physical effect of a current passing through an electrical conductor producing thermal energy is known as Joule heating. This thermal energy is then manifested as an increase in the temperature of the conductor material. The process of Joule

heating effect can be seen in electric oven, electric kettle and room heaters etc.

1.15 Porous media

A porous medium is a solid matrix with enough open space or voids which enable the movement of fluid particles. Rock, soil, sand, biological tissues, and sponge are some examples of porous media. A porous media is usually characterized by its porosity and permeability. Porosity is the ratio of the volume of open space to the volume of the solid matrix including open space. The value usually lies between 0 and 1. Permeability depends on the geometry or structure of the medium. Fuel cells, petroleum engineering, filtration, and soil mechanics utilize the concept of porous media.

1.15.1 Darcy's Law

Fluid filtration through a porous medium can be mathematically expressed by the Darcy law. Oil, gas, and water flow through petroleum reservoirs are described with the help of the Darcy law. It is valid for laminar and low viscous cases. Darcy's law (1856) found a proportionality between the applied pressure and flow rate. In the case of the isotopic medium, Darcy's law is mathematically expressed as $\nabla P = -\frac{\mu}{K_p}\, v$, (see (Nield et al., 2006)) where μ is the dynamic viscosity of fluid, K_p (a scaler in isotropic medium) is the permeability of the medium, v is the velocity and P is the pressure.

Table 1.1: *Porosity and permeability of some common materials Based on data by (Bejan & Lage, 1991) and (Nield et al., 2006)*

Material	**Porosity**	**Permeability,**$K_p(cm^2)$
Brick	0.12 -0.34	$4.8 \times 10^{-11} - 2.2 \times 10^{-9}$
Soil	0.43-0.54	$2.9 \times 10^{-9} - 1.4 \times 10^{-7}$
Sand	0.37-0.50	$2 \times 10^{-7} - 1.8 \times 10^{-6}$
Leather	0.56-0.59	$9.5 \times 10^{-10} - 1.2 \times 10^{-9}$

1.15.2 Brinkman's equation

Brinkman (Brinkman, 1949) modified Darcy's law in 1949 using a Laplace term which is significant for the flow around a particle submerged in a porous medium with the no-slip condition. It is suitable for a high porous medium (porosity $>$ 0.6) with negligible convective inertia. Porosity is normally less than 0.6 in a naturally occurring porous medium. Brinkman's equation is mathematically expressed as

$$\nabla P = -\frac{\mu}{K_p} v + \mu \nabla^2 v \tag{1.15.1}$$

where μ is the effective viscosity.

1.15.3 Darcy Forchheimer flow

Darcy-Forchheimer flow is a fluid flow through a porous medium satisfying the Darcy-Forchheimer relation that subsumes inertial properties and boundary characteristics. A Laminar flow observed in the low fluid velocity through porous medium with Reynolds number is less than or equal to 1. A sudden transition of laminar to turbulent flow does not happen when the Reynolds number is augmented between 1 to 10. In such a case surface drag due to solid obstacles is comparable with surface drag due to friction (see (Nield et al., 2006)). Darcy Forchheimer equation is mathematically expressed as (see (Joseph, Nield, & Papanicolaou, 1982))

$$\nabla P = -\frac{\mu}{K_p} v - \frac{C_f}{\sqrt{K_p}} \rho_f \ |v| \, v \tag{1.15.2}$$

where C_f is drag constant and ρ_f is density. The last term in the expression is called the Forchheimer term.

1.16 Boussinesq approximation

The Boussinesq approximation is a significant method utilized in nonisothermal problems and natural convection processes. The approximation is more accurate in low-density variations. It accounts for the importance of density variation in the buoyancy term (ρg). If ρ_0 is the reference density then

$$(\rho - \rho_0) \, g = -\rho_0 \ \beta_T \, (T - T_0) \, g. \tag{1.16.1}$$

Where T is the temperature, T_0 is the reference temperature and β_T is the coefficient of thermal expansion. When heat and mass transfer effects co-exists in a system then the Boussinesq approximation is

$$(\rho - \rho_0)\, g = -\rho_0\ \beta_T\ \ (T - T_0)\, g - \rho_0\ \beta_C\, (C - C_0)\, g \tag{1.16.2}$$

Where β_C is the coefficient of species expansion and C_0 is the reference Concentration.

1.17 Basic equations describing the fluid flow

1.17.1 Equation of continuity (Conservation of mass)

Equation of continuity is based on the principle of law of conservation of mass which is defined as the rate of generation of mass within a given volume is equal to the difference between the rate of mass entering into a volume and the rate of mass out of the volume. Continuity equation can be mathematically expressed as

$$\frac{\partial \rho}{\partial t} + div\,(\rho V) = 0. \tag{1.17.1}$$

where $V = (u, v, w)$ are the components of velocity in x, y, and z directions. $div\,(\rho V) = 0$, if the fluid is steady and compressible. $div\,(V) = 0$, if the fluid is steady and incompressible.

1.17.2 Navier -Stoke's equations (Conservation of momentum)

Navier -Stoke's equation is based on Newtons' second law of motion which states that the total force is equal to the rate of change of linear momentum.

$$\rho \frac{DV}{Dt} = \rho\ F + \mu\ \nabla^2 V - \nabla P. \tag{1.17.2}$$

$\frac{D}{Dt} \cong \frac{\partial}{\partial t} + (V.\nabla)$ is know as the material derivative.

1.17.3 Conservation of energy

The equation of energy is based on the law of conservation of energy which states that the total energy in an isolated system is constant. Rate of increase of energy in a volume is equal to the difference of rate at which heat is produced by the work (due to surface stress & external agencies) and rate of energy loss (due to conduction & convection).

$$\rho C_p \frac{DT}{Dt} = \frac{\partial Q}{\partial t} + k \frac{\partial}{\partial x_i} \left(\frac{\partial T}{\partial x_i} \right) + \varphi_v. \tag{1.17.3}$$

where $\varphi_v = \mu \left(\frac{\partial v_i}{\partial x_j} + \frac{\partial v_j}{\partial x_i} \right) \frac{\partial v_i}{\partial x_j}$ is the dissipation function, a heat generation function due to frictional forces.

1.18 Dimensional analysis & Non dimensional parameters

Dimensional analysis is a mathematical tool for obtaining the qualitative behaviour of a physical problem. In dimensional analysis, basic equations are converted into dimensionless forms involving non-dimensional parameters. The ratio of one force to the other force yields a dimensionless number known as the non dimensional parameter. The dimensionless parameter (non dimensional parameters) aids us in comprehending the physical significance of a specific phenomenon associated with the problem. Major non dimensional parameters in the thesis are

1.18.1 Magnetic parameter or Hartmann number

Hartmann number is a dimensionless number that is defined as the ratio of an electromagnetic force to viscous force. Lorentz force generates due to an increase in Hartmann number that influences the flow profiles of an electrically conducting fluid passing through a magnetic field. Mathematically it can be denoted as.

$$M = B_0 l \sqrt{\frac{\sigma}{\mu}} \tag{1.18.1}$$

where B_0 is magnetic field intensity, l is the characteristic length scale, σ is the electrical conductivity and μ is dynamic viscosity.

1.18.2 Schmidt number

Schmidt number is a dimensionless number that is defined as the ratio of momentum diffusivity to mass diffusivity. It is used to characterize fluid flows that have both momentum and mass diffusion convection processes going on at the same time. Mathematically it can be represented as.

$$Sc = \frac{\nu}{D} \tag{1.18.2}$$

where ν is the kinematic viscosity and D is the mass diffusivity.

1.18.3 Reynolds number

Reynolds number is a dimensionless number that is defined as the ratio of inertial force to viscous force. Reynolds number determines the flow pattern. A high Reynolds number enhances the inertial force and produces a turbulent flow pattern. Laminar flow takes place at a low Reynolds number. Viscous forces dominate in the case of small Reynolds numbers. Mathematically, it can be expressed as

$$Re = \frac{ul}{\nu} \tag{1.18.3}$$

where u is the flow speed, l is the characteristic length scale and ν is the kinematic viscosity

1.18.4 Eckert number

Eckert number is a dimensionless number that is defined as the ratio of advective mass transfer to the heat dissipation potential. It characterizes the Self- heating of a fluid due to viscous dissipation. Mathematically, it can be represented as

$$Ec = \frac{U_W^2}{C_p\left(T_w - T_\infty\right)} \tag{1.18.4}$$

where U_W is the velocity at the wall, C_p is the specific heat at constant pressure, (T_w, T_∞) denotes temperatures at the wall and away from the wall, respectively.

1.18.5 Prandtl number

Prandtl number is a dimensionless number that is defined as the ratio of momentum diffusivity to thermal diffusivity. Pr is connected with the heat convection process. For example, $Pr = 0.015$ is for liquid mercury and Pr varies between 100 & 40000 for Engine oil. Liquid mercury show more thermal diffusivity than engine oil. In addition, heat convection is more effective in engine oil than liquid mercury. Mathematically, it can be expressed as

$$\mathrm{Pr} = \frac{\mu C_p}{k} \tag{1.18.5}$$

where μ is the dynamic viscosity, C_p is the specific heat at constant pressure and k is the thermal conductivity.

1.18.6 Grashof number

Grashof number is a dimensionless number that is defined as the ratio of the buoyancy to viscous force. The number occurs in the natural convection process. In the presence of buoyancy force, thermal and solutal Grashof numbers are significant. As the temperature increases, the density decreases and the fluid rises. The motion is caused by the buoyancy force. Thermal and solutal Grashof numbers emerge due to temperature and concentration gradient, respectively. Mathematically, thermal and solutal Grashof numbers are described as follows

$$G_r = \frac{\nu g \beta \left(T_0 - T_d\right)}{U_0 {w_0}^2}. \tag{1.18.6}$$

$$G_m = \frac{\nu g \beta \left(C_0 - C_d\right)}{U_0 {w_0}^2}, \tag{1.18.7}$$

where β is the volume expansion coefficient, g is the acceleration due to gravity, ν is the kinematic viscosity, (T_0, T_d) is the temperature of the fluid near the origin and at d respectively. (C_0, C_d) is the concentration of the fluid near the origin and at d respectively.

1.18.7 Biot number

Biot number is a dimensionless number that is defined as the ratio of thermal resistance inside a body and at the surface of the body. The number describes the temperature variations inside a body during the heating and cooling process over the surface. Mathematically it can be expressed as

$$Bi = \frac{h}{k}\, l \tag{1.18.8}$$

where h is convective heat transfer coefficient, k is the thermal conductivity, and l is the characteristic length scale.

1.18.8 Soret number

Soret number is a dimensionless number that is defined as the ratio of thermal diffusion coefficient and the normal diffusion coefficient. It measures the degree of separation of the species. Mathematically, it can be expressed as

$$S_0 = \frac{D_m K_T \left(T_W - T_\infty\right)}{T_m \nu_f \left(C_W - C_\infty\right)} \tag{1.18.9}$$

where $D_m, K_T, T_W, T_\infty,\ C_\infty$ and ν_f are mass diffusivity, thermal diffusion ratio, temperature near the solid boundary, temperature far away the solid boundary, free stream concentration and kinematic viscosity, respectively.

1.18.9 Weissenberg number

Weissenberg number is a dimensionless number that is defined as the ratio of the elastic force to the viscous force. Elastic effects dominate the viscous force if the time scale of flow is less than the relaxation time and vice versa. So, the Weissenberg number has a significant role in the study of viscoelastic flows. Mathematically, it can be described as

$$We = \frac{\tau_{xx} - \tau_{yy}}{\tau_{xy}} \tag{1.18.10}$$

1.18.10 Nusselt number

The conductive and convective heat transfer phenomenon occurs through a fluid layer of thickness l. According to Newton's law, the mathematical notation of heat flux (in the case of convection) is

$$q_{conv} = h\delta T. \tag{1.18.11}$$

where h is the convective heat transfer coefficient and δT is the temperature difference of the fluid layer.

According to Fourier's law, the mathematical expression of heat flux (in the case of conduction) is

$$q_{cond} = \frac{k\delta T}{l} \tag{1.18.12}$$

where k is thermal conductivity.

A Nusselt number is a dimensionless number that is defined as the ratio of convective to conductive heat transfer. The Nusselt number can be used to estimate the effectiveness of heat convection at the surface. Mathematically, it can be expressed as

$$Nu = \frac{hl}{k} \tag{1.18.13}$$

where h is convective heat transfer coefficient, l is the characteristic length and k is thermal conductivity.

1.18.11 Sherwood number

Sherwood number is a dimensionless number that is defined as the ratio of convective mass transfer to diffusive mass transfer rate. The Sherwood number can be used to estimate the effectiveness of mass convection at the surface. Mathematically, it can be represented as

$$Sh = \frac{k_m l}{D_m}, \tag{1.18.14}$$

where k_m is the convective mass transfer coefficient, l is the characteristic length scale and D_m is the mass diffusivity.
Solution diffuses from a higher concentration to a lower concentration region and the diffusion flux is proportional to the concentration gradient. According to Fick's law, diffusion flux is given by

$$J = -D\frac{dC}{dx} \tag{1.18.15}$$

where D is the diffusion coefficient, C is the concentration and x is the position.

1.18.12 Skin friction coefficient

The fluid velocity at the touching surface is zero whereas it is maximum in the main stream of the flow. The boundary layer of the flow is the region where the fluid velocity starts from zero to maximum. A skin friction coefficient is a non-dimensional number that estimates the tangential shear force of a moving fluid against the surface. Tangential shear force is due to no-slip conditions caused by viscosity, geometry, and the type of fluid flow. Mathematically, it can be expressed as

$$c_f = \frac{\tau_w}{\rho U_\infty^2} \tag{1.18.16}$$

where τ_w is the local shear wall stress, U_∞ is the free stream velocity.

1.19 Nanofluid

The performance of a fluid in the heat transfer phenomenon significantly depends on the thermophysical properties of the fluid. Metal and metal oxides show higher thermal conductivity than fluids. Dispersion of these nanometer-sized (1 nm to 100 nm) particles in the conventionally used fluids like water, Ethylene glycol and

oil, etc, revolutionised the area of fluid mechanics. These colloids are known as nanofluids. Nanoparticles can be metal-based (Cu, Ag, Au, Zn), metal oxide-based (Fe_3O_4, Al_2O_3, TiO, ZnO, CUO), carbide based (Calcium carbide, Silicon carbide) Nitride based (Aluminium nitride, Silicon nitride), Sulfide based (Zinc sulfide, Silver sulfide), carbon-based (Graphene, Carbon nanotubes), or polymer-based (Polystyrene). Nanofluid is prepared by dispersing a small quantity of nanoparticles in base fluid which can significantly alter the properties of the base fluid. Water-based, Glycol-based, oil-based (vegetable oil, gasoline, kerosene, and lubricating oil) or Refrigerant-based (R134a , R600a, R141b) base fluids are commonly used in Engineering and industrial applications. Further, the performance of a nanofluid is influenced by the volume fraction of nanoparticles, particle shape, particle size and temperature.

1.19.1 Volume fraction of nanoparticles

The nanoparticle volume fraction is the ratio between the volume of nanoparticles and the volume of all constituents of the mixture. Mathematically, nanoparticle volume fraction is expressed as $\phi = \frac{V_{np}}{V_{nf}} = \frac{V_{np}}{V_{np}+V_{bf}}$ where V_{np}, V_{nf}, and V_{bf} represent the volume of nanoparticle, nanofluid, and base fluid respectively (see (A. R. I. Ali & Salam, 2020)). Metals and metal oxides show larger thermal conductivity in comparison with fluids. Nanofluid was first discovered by Choi (Choi & Eastman, 1995) for its exceptional cooling performance and heat transfer ability. Base fluid and nanoparticles in nanofluid exhibit unique chemical and physical properties.
Major applications of nanofluids are

- Magnetic liquid rotatory seal utilizes the properties of magnetic nanoliquids and operates with low maintenance in the industry.
- The efficiency of solar thermal collectors enhances with the use of nanofluid as the absorption media.
- Nanofluids can reduce friction and grinding force with the help of a dense slurry layer in the grinding process of cast iron.
- Non-toxic nanoparticles(like gold nanoparticles) can work as a drug delivery agent.

- Nanoparticles can cross the cell membrane of the bacteria and work as an antibacterial agent.
- Nanofluids can reduce the size of submarines, fighter jets, etc. by contributing towards smaller and efficient cooling system.
- Apart from these nanofluids are used in vehicle brake fluids, heat exchangers, nuclear reactors, transformer oil, refrigeration and electronics equipment.

1.19.2 Thermophysical properties of nanofluid

Density of nanofluid

The ratio of mass to volume is the density. According to classical mixture law, the density of nanofluid is

$$\rho_{nf} = \rho_s \phi + (1 - \phi)\, \rho_f. \tag{1.19.1}$$

Specific heat of nanofluid

Specific heat of a substance is the quantity of heat required to change the temperature by one degree. Specific heat of nanofluid is (see (Xuan & Roetzel, 2000))

$$(\rho C_p)_{nf} = (\rho C_p)_s \phi + (1 - \phi)\, (\rho C_p)_f. \tag{1.19.2}$$

Thermal conductivity of nanofluid

The Maxwell model for spherical shape nanoparticles and the Hamilton-Crosser model for non-spherical shape nanoparticles are the two most commonly used models for thermal conductivity in the literature.
The Maxwell model predicts that the thermal conductivity of nanofluid is

$$\frac{k_{nf}}{k_f} = \frac{k_s + 2k_f + 2\phi\,(k_s - k_f)}{k_s + 2k_f - \phi\,(k_s - k_f)} \tag{1.19.3}$$

The Hamilton-Crosser model (Hamilton & Crosser, 1962) for thermal conductivity of nanofluids is

$$\frac{k_{nf}}{k_f} = \frac{k_s + (\mathcal{H} - 1)\, k_f - (\mathcal{H} - 1)\, \phi\, (k_f - k_s)}{k_s + (\mathcal{H} - 1)\, k_f + \phi\, (k_f - k_s)} \tag{1.19.4}$$

. where $\mathcal{H} = \frac{3}{\psi}$ where ψ is the sphericity and $\mathcal{H}$ is the empirical shape factor.

Dynamic viscosity of nanofluid

Two of the most commonly used effective dynamic viscosity models are the Brinkman and Einstein models. The Brinkman model (Brinkman, 1952) is $\frac{\mu_{nf}}{\mu_f} = \frac{1}{(1-\phi)^{2.5}}$ and the Einstein model is $\frac{\mu_{nf}}{\mu_f} = 1 + 2.5\ \phi$ (see (Drew & Passman, 2006)).

1.19.3 Shape and size of nanoparticles

Effective dynamic viscosity and thermal conductivity of nanofluid depend on the shape and size of nanoparticles. The shape of nanoparticles may be spherical, cylindrical, brick, platelet, or blade. (Timofeeva et al., 2009) studied particle shape effect on the rheological properties of Al_2O_3/EG-water. In a similar way size of nanoparticles influenced the thermal conductivity and viscosity of nanofluids. (Teng, Hung, Teng, Mo, & Hsu, 2010) found an enhanced thermal conductivity of Al_2O_3/water nanofluid with a decrease in particle size of nanoparticles.

1.20 Solution methodology

In the research, the following tools have been opted for the numerical computation

1.20.1 Perturbation technique

Perturbation technique is an analytical method for finding approximate solution of nonlinear differential equations. They are more suitable for recurring solutions of vibrating systems involving nonlinear effects and complex boundary conditions. In the perturbation technique a small parameter $\epsilon < 1$ is added to the mathematical description of the solvable problem. Analytical solution can be expressed as $u(x,t) = u_0(x) + \sum_{i=1}^{\infty} \epsilon^i u_i(x,t)$. The higher order terms are known as perturbation terms. The series is a convergent series that converges to a limit as ϵ tends to zero (see (Singh & Kumar, 2009)).

1.20.2 Finite difference method based bvp5c Routine

The bvp5c solver integrates simultaneous differential equations of the form $y' = f(x,y)$ with initial/boundary conditions. It starts with an initial guess and works with an algorithm based on the four-stage finite difference code Lobatto IIIa formula (see (Kierzenka & Shampine, 2008)). The flowchart of the numerical simulation is given in the Figure 1.2.

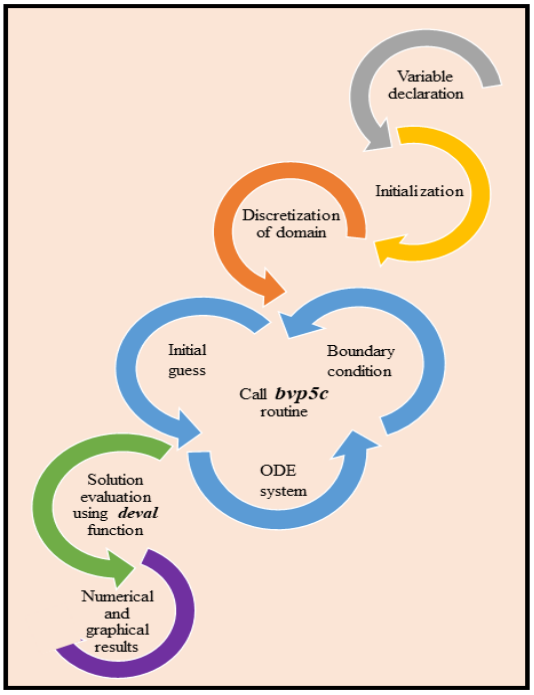

Figure 1.2: *Flow chart depicting bvp5c routine*

1.20.3 Runge–Kutta method

The fourth order Runge–Kutta method is used to find an approximated value of y at x. Nonlinear ordinary differential equations are converted to a system of first order ODEs for the solution procedure. The Runge–Kutta algorithm is described as follows:- $x_i = x_{i-1} + h$.

$y_{i+1} = y_i + \frac{1}{6}(K_1 + 2K_2 + 2K_3 + K_4)$.

$K_1 = h\ f(x_i, y_i)$.

$K_2 = hf\left(x_i + \frac{h}{2}, y_i + \frac{K_1}{2}\right)$.

$K_3 = hf\left(x_i + \frac{h}{2}, y_i + \frac{K_2}{2}\right)$.

$K_4 = hf(x_i + h\ , y_i + K_3)$.

1.20.4 Shooting method

The shooting method is a numerical technique that solves a boundary value problem (BVP) by reducing it into an initial value problem (IVP). For this, an initial guess value is assumed for the unknown initial conditions. The newly derived IVP is solved and checked for accuracy by comparing the solution with the existing boundary conditions. If the accuracy of the solution is less than the desired accuracy level, the process is repeated by choosing a new guess value. For this, methods like the

midpoint rule, Newton-Raphson method, etc. are utilized.

1.20.5 Bulirsch-Stoer method

The Bulirsch-Stoer algorithm is a numerical procedure based on the Richardson extrapolation and the midpoint method (See (Kiusalaas, 2005) and (Bulirsch, Stoer, & Stoer, 2002)). The midpoint formula $y(x+h) = y(x-h) + 2hf[x, y(x)]$ of the numerical integration of $y' = f(x, y)$ is the basis of the Bulirsch-Stoer method. The midpoint method is initially applied in two steps. With each successive integration, the number of steps is increased by two, and each integration is followed by Richardson extrapolation. When two successive solutions differ by less than a prescribed tolerance, the procedure is terminated. For improved efficiency, the automated step size modification has been removed from the classical Bulirsch and Stoer technique algorithm. The Bulirsch-Stoer method is advantageous in computations that require high accuracy solutions for smooth functions. The high accuracy, simplistic approach, easy execution, and improved efficiency provide an upper hand for the Bulirsch-Stoer method over the existing numerical techniques.

1.21 Statistical analysis

1.21.1 Correlation with probable error and regression analysis

Correlation is a statistical technique that quantifies the nature of the association of two variables. The relation between two variables is a positive or a negative correlation depending on their sign. A positive correlation means that an increment in one variable leads to an increase in the other. The magnitude of r_c indicates the intensity of this relationship. Correlation is said to be significant if $\left|\frac{r_c}{PE}\right| > 6$; where $PE = 0.6745\ \left(\frac{1-{r_c}^2}{\sqrt{\tilde{n}}}\right)$ and $\tilde{n}$ is the total observation number (see (Fisher et al., 1921)). PE is known as probable error. It establishes the reliability of the correlation coefficient. The probable error gives an idea of how to generalise the correlation coefficient calculated from the sample to the population.

Regression analysis is a statistical modelling technique used to establish a relationship between a dependent and one or more independent variables. The following elements are included in a multilinear regression model: independent variables, dependent variables, unknown parameters and error terms. Mathematically, it can be expressed as: $Y = r_i X_i + e\ ,\ i = 1\ to\ n$ where Y is dependent variable, X_i are independent

variables and e is the error term.

1.22 Response surface methodology (RSM)

RSM is an experimental design-based statistical technique that illustrates the impact of influential parameters (independent variables) and their interactive effects on the physical quantity of choice (dependent or response variable). Experimental trials are time-consuming and costly whereas RSM reduces the number of trials and optimizes the response variable. RSM using the Central Composite Design (CCD) is a suitable sequential experimentation method which is incorporated in the present study with 20 ($2^j + 2j + o,\ j\ = 3, o = 6$) runs, here o denotes the number of faces and j denotes the number of factors. The relation involves 2^3 factorial 6 center and 6 axial points (see (Mahanthesh, Mackolil, & Mallikarjunaiah, 2021)). A full quadratic 3 level factorial design is adopted in the study as follows

$$\begin{aligned} \textit{Response}\ (Y) = \ & L_1X_1 + L_2X_2 + L_3X_3 + L_4X_1X_2 + L_5X_2X_3 + L_6X_1X_3 \\ & + L_7X_1^2 + L_8X_2^2 + L_9X_3^2 + L_{10}. \end{aligned} \tag{1.22.1}$$

where, L_i ($i = 1,\ 2,\ \ldots,\ 10$) denote the regression coefficients. The RSM technique becomes advantageous in finding the levels of the parameters that optimize the response. ANOVA table as described evaluates the quality of the fitted quadratic model reliably. The significance of linear, quadratic, and interactive regression terms are computed statistically using F and p values. All the regression terms with a high F and p-value < 0.05 in the fitted model are significant.

1.23 Sensitivity analysis

Sensitivity is a measurement that interprets the level of change in response variables with variation in independent variables. The positive or negative sign in the sensitivity function indicates the nature of the sensitivity and its magnitude delineates the intensity of the relationship (see (Mackolil & Mahanthesh, 2021a)).

1.24 Literature review

1.24.1 Magnetohydrodynamics

The concept of magnetohydrodynamics (MHD) was introduced by Hannes Alfven in 1942. Naturally convected magnetohydrodynamic flow has been studied by

many researchers theoretically and experimentally having applications in scientific, engineering, industrial and medical fields. It plays a pivotal role in the field of microelectronics, solar technology, glass fibers, hot rolling, paper production, and plasma studies (see (Vinita & Poply, 2020), (Rabbi et al., 2020) and (Alsagri, Hassanpour, & Alrobaian, 2019)). (Naga Santoshi, Venkata Ramana Reddy, & Padma, 2019) studied Magneto Carreau nanofluid numerically under slip and obtained suppressed velocity profiles through augmented values of Hartmann number. (Abbas, Rehman, Shah, Idrees, & Qayyum, 2020) analysed magneto hydrodynamic flow on a stretching sheet using Carreau fluid. They deployed a Runge-Kutta 4th order method for solving the problem numerically. (Gholinia, Armin, Ranjbar, & Ganji, 2019) studied the influence of magnetic field over an expanding cylinder utilizing CNT nanofluids. With increasing magnetic field parameter a decrease in the surface drag was observed. (Bilal, Sagheer, & Hussain, 2018) numerically examined the MHD flow over a lengthening cylinder on Williamson fluid and noticed a decline in velocity profile due to an augmentation in magnetic field parameter. (Sohail & Naz, 2020) incorporated a revised mass and heat transmission model in MHD flow over a stretched cylinder and attained the numerical solutions using OHAM method. Further, Magnetohydrodynamics (MHD), has relevance in drug targeting, metallurgy, polymer industry, plasma jet, electromagnetic pump, aeronautics, fusion reactors, crystal growth, and MHD flow meters. (Hayat, Riaz, Aziz, & Alsaedi, 2020) scrutinized the hydromagnetic nanoliquid flow past a lengthening surface. They noticed an elevation in the thermal profile and a decline in the velocity profile with augmented values of Hartmann number. The consequence of uniform magnetic force and ellipse-shaped obstacle on the nanoparticle migration within a porous cubic cavity was elucidated by (Sheikholeslami, Shah, Shafee, Khan, & Tlili, 2019). (Shehzad, Sheikholeslami, et al., 2020) illustrated that mounting values of the Hartmann number declined the heat transfer characteristics by 11.97 %. Magnetic nanoparticles have applications in cancer therapy, drug delivery, magnetic cell separation, and magnetic resonance imaging (see (P. S. A. Reddy & Chamkha, 2018) and (Salehi, Nori, Hosseinzadeh, & Ganji, 2020)). (O. D. Makinde et al., 2018) analyzed the significance of radiation and heat sources on the MHD flow over a rotating disk involving aluminium and titanium alloy nanoparticles. (Ouyang et al., 2020) remarked an enhancement in the drag coefficient with increasing magnetic

field parameter. (Salahuddin, Sakinder, Alharbi, & Abdelmalek, 2021) deliberated a hydromagnetic nanofluid flow towards a heated sphere and observed a decline in the nanofluid velocity with augmenting values of magnetic field parameter.

1.24.2 Nanofluid

In the 19th century, there was a high demand for innovative methodologies in finding an efficient thermal conducting fluid due to its various industrial applications. Low thermal conductivity of conventional fluids like water, ethylene-glycol, biological fluids, glycol, and oil limited their functionality. Metals and metal oxides show larger thermal conductivity in comparison with fluids. Nanofluid was first discovered by (Choi & Eastman, 1995) for its exceptional cooling performance and heat transfer ability in 1995. The researchers investigated a new class of fluids by suspending nanometer-sized (1 nm to 100 nm) copper metallic particles in water. Later, researchers investigated different nanofluids by suspending various nanoparticles (metalic or non metalic) in conventional fluids. Base fluid and nanoparticles in nanofluid exhibit unique chemical and physical properties (see (Chamkha, Jena, & Mahapatra, 2015)). Concerning the heat transfer property of nanofluid, (Eastman, Choi, Li, Thompson, & Lee, 1996) observed that when 5% of Copper Oxide nanoparticles was used in water, the heat transfer property increased by 60 %. Nanofluids are used in solar thermal collectors, heat pipes, automotive radiators and tube heat exchangers (see (Leong et al., 2018)). Further, nanofluids exhibited a higher thermal conductivity when compared with the traditional fluids. Nanofluids play a crucial role in cooling systems, hydraulic systems, biomedical equipment, and nuclear reactors (see (Ho, Cheng, Yang, Rashidi, & Yan, 2021), (Sheriff, Mir, Ahmad, & Rafiq, 2021), (Deymi-Dashtebayaz et al., 2021), (Abdo & Saidani-Scott, 2021) and (Erkan, Tüccar, Tosun, & Özgür, 2021)).

1.24.3 Hybrid nanofluid

Hybrid nanofluid is a colloidal suspension of base fluid with more than one distinct nanoparticle. Hybrid nanoliquids due to their superior heat transfer capabilities have applications in solar collectors, heat exchangers, nanomedicines, and electronic cooling devices. (Tahat & Benim, 2017) experimentally analyzed the thermal conductivity and viscosity of Al_2O_3-CuO/ethylene glycol hybrid nanoliquid and observed a significant increase in these parameters with respect to volume fraction of

nanoparticles. (Shahul Hameed, Suresh, & Singh, 2019) reported that a 0.3% volume fraction of Al_2O_3-Cu/water nanofluid enhanced the heat transfer coefficient by 20.48 % when compared with water. Further, a thermal enhancement of 6-11% for CuO-Al_2O_3/water nanofluid in comparison with alumina nanoliquid was experimentally derived by (Plant, Hodgson, Impellizzeri, & Saghir, 2020). More studies concerning hybrid nanoliquid flow can be seen in (Khashi'ie, Arifin, Merkin, Yahaya, & Pop, 2021), (Gangadhar, Bhargavi, Kannan, Venkata Subba Rao, & Chamkha, 2020) and (Mathew, Neethu, & Areekara, 2021).

1.24.4 Channel flow

(Sheikholeslami, Hatami, & Ganji, 2013) conducted an analytical study of hydromagnetic flow in a porous channel and discovered an inverse relationship between the thickness of the velocity boundary layer and the Reynolds number. (Gul, Khan, Shafie, Khalid, & Khan, 2015) investigated the flow of ferro nanofluid through a vertical channel and its heat transfer effects. The researchers also conducted a velocity comparison between Al_2O_3/water and Fe_3O_4/water nanofluids. (Raza, Rohni, & Omar, 2016) investigated MHD flow through a porous channel with stretching effects. Skin friction decreased as the volume fraction increased, according to the researchers. MHD convective flow through an inclined channel can be found in (Malashetty & Umavathi, 1997), (Said, Habib, Badr, & Anwar, 2005), (Hasnain, Abbas, & Sajid, 2015) and (S. Hussain, Mehmood, Sagheer, & Farooq, 2017).
(S. Das, Jana, & Makinde, 2016) reviewed the transient free convection nanofluid flow through a vertical channel in the presence of thermal radiation. Convection flow through the vertical channel is decisive in the cooling systems of heat exchangers and solar cells. Warm blood circulation in mammals and engine cooling are examples of convection. Forced and free convections are very important in the convection flows. Enforced convection with heat transfer properties in a porous channel is evaluated by (Maghrebi, Nazari, & Armaghani, 2012). An oscillatory MHD flow through a rotating channel in the presence of Hall current has been analyzed previously by (Pal & Talukdar, 2013). Electrically conducting fluid flow through a rotating porous channel has wide industrial uses like nuclear reactors, geothermal systems and filtration etc. (See (Sulochana et al., 2014)).

1.24.5 Flow past a flat plate

Flow past a flat plate frequently occurs in the field of aerodynamics, plasma studies, and cooling systems. Fluid flow over an inclined/vertical flat plate encounters buoyancy forces which significantly affect the convective flow and heat transfer. Free and forced convection is important in such flows. Free convective flow past a vertical plate is discussed in (Krishna & Chamkha, 2019), (Nandi & Kumbhakar, 2020), (Krishna, Swarnalathamma, & Chamkha, 2019) and (Akcay, Akdag, & Palancioglu, 2020). (Krishna et al., 2019) studied the mixed convective flow over a flat plate and found that frictional force at the plate was decreased due to an increase in the applied magnetic field. (Akcay et al., 2020) experimentally investigated the mixed convective fluid flow over a vertical flat plate. The researchers observed that heat flux on the plate significantly affected the performance of heat transfer. (Khademi, Razminia, & Shiryaev, 2020) studied the mixed convective fluid flow over an inclined plate. They implemented the Differential Quadrature Method (DQM) for solving the nonlinear differential equations. (Mondal, Pal, Chatterjee, & Sibanda, 2018) explored the MHD mixed convective fluid flow over an inclined plate. It is found that the velocity profile is declined due to an increase in the inclination angle. (Rashed, Ahmed, & Sheremet, 2019) investigated the MHD flow over an inclined plate in the presence of solar radiation. The researchers noticed an enhancement in the temperature field by the increment in the angle of inclination.

1.24.6 Flow past a stretching sheet

Stretching surface has intrigued many researchers due to its diverse applications in industrial and engineering fields like production of plastic and rubber plates, cooling of metallic plate in a bath, metal extrusion, etc. (J. A. Khan, Mustafa, Hayat, & Alsaedi, 2014) studied the heat transfer over a bilateral stretched nonlinear surface numerically with the aid of OHAM and Runge-Kutta coupled with shooting method. (Z. Hussain, Hayat, Alsaedi, & Ahmad, 2018) analysed the effect of heat generation of CNTs nanofluids over a nonlinear bilateral stretched surface. A reduced thermal layer due to the rate of stretching was noted. (M. Nandeppanavar & Siddalingappa, 2013) analysed the consequence of thermal radiation and viscous dissipation on heat transfer over a nonlinear stretching sheet through a porous medium and inferred a positive and negative effect on temperature due to Eckert number and

thermal radiation parameter, respectively. (Tlili, Bilal, Qureshi, & Abdelmalek, 2020) investigated three dimensional flow over a stretched surface using Williamson fluid and they had established that the velocity along Y direction enhanced due to stretching. (Hayat, Aziz, Muhammad, & Alsaedi, 2019) investigated the Carreau nanofluid flow induced by a bilateral stretched surface. They tackled the nonlinear differential equations using NDsolve. (Shakunthala & Nandeppanavar, 2019) studied the boundary layer flow and Cattaneo-Christov heat flux of a nonlinear stretching sheet with suspended carbon nanotubes.

1.24.7 Flow past a stretching cylinder

Viscous fluid flow over an expanding cylinder has important applications in industry and engineering fields. Production of plastic films, rubber, copper wires, and paper are some industrial applications of viscous fluid flows. The heat transfer rate and stretching determines the quality and finishing of a product. Nanofluid flow over a lengthening cylinder with shape factor is considered in the study of (Shaiq, Maraj, & Iqbal, 2019). Heat transfer via a stretched cylinder utilizing nanofluids is important in food processing, glass fibre production and metal spinning. (Shojaei, Amiri, Ardahaie, Hosseinzadeh, & Ganji, 2019) analysed second-grade non-Newtonian fluid flow over a stretched cylinder and observed an elevated temperature profile due to large curvature parameter values. (Z. Hussain, Hayat, Alsaedi, & Ahmed, 2018) conducted a simultaneous study on the nanofluid flow over an elongating cylinder and a flat sheet. They noticed an increase in the velocity profile due to flow over a flat sheet when collated with flow over an expanding cylinder.

1.24.8 Flow past a rotating disk

Following (Von Kármán, 1921) pioneering work, the fluid motion caused by disc spinning has stimulated the interest of many researchers due to its wide application in engineering and industry. Von Kármán flow delineates a swirling flow by the uniform rotation of a disk. Centrifugal pumps, polymer extrusion, disk drives, electrochemistry, petroleum processes, evaporators, and lubrication are some applications that utilize the concept of rotational fluid flow (see (M. I. Khan, 2021) and (Shehzad, Mabood, Rauf, & Tlili, 2020)). (S. Mandal & Shit, 2021) scrutinized the mechanism of nanoliquid flow past a rotating disk and the researchers noticed a strong relationship between the rate of heat transfer and rotation of the disk.

(Tassaddiq et al., 2020) explored nanoliquid flow past a rotating disk and they found enhanced velocity and temperature profiles by rotation of the disk. (Ibrahim, 2020) numerically analyzed viscous fluid (time-dependent) flow over a rotating disk and observed a decrease in volume fraction of nanoparticles as the Schmidt number increased.

1.24.9 Heat source

Heat source/sink parameter has a key role in medical and industrial field. Heat pumps, heat exchangers and filtration device are a few examples exploiting the effect of various heat sources. Nanofluid flow over an elongating cylinder with heat source is reviewed in (A. Ahmed, Khan, Hafeez, & Ahmed, 2020) and (M. Ali, Shahzad, Sultan, & Khan, 2020). (Gireesha, Nagaraja, Sindhu, & Sowmya, 2020) studied about the CNT nanofluid flow on top of a curved elongating sheet and noticed an increase in temperature due to exponential space-based heat source (ESHS). (Mahanthesh, Shashikumar, & Lorenzini, 2021) scrutinized the simultaneous effect of ESHS and linear heat source (LHS) parameter on the nanofluid flow over a stretchable rotating disk. They discovered an elevated heat transfer rate due to ESHS parameter than the LHS parameter. Non-Newtonian and Newtonian fluid flow considering ESHS for different scenarios are studied by (Mahanthesh, Shashikumar, Gireesha, & Animasaun, 2019) and (Nagaraja & Gireesha, 2021). Heat sources have a remarkable role in the regulation of heat fluctuations in thermal systems. (Pattnaik, Mishra, Mahanthesh, Gireesha, & Rahimi-Gorji, 2020) numerically computed the effect of the exponential heat source (EHS) on fluid flow over a plate and compared it with thermal based-heat source (THS).

Heat source parameters can regulate heat transfer effects which have a key role in space heating, air conditioning, and industries including rubber, polymer, food, oil production, etc. Heat source from a high surface area naturally generates an irregular (non-uniform) heat distribution (Fauzan, Muyeen, & Islam, 2021). Temperature-dependent and space-dependent heat source models are described in the previous studies (Mabood, Ibrahim, Rashidi, Shadloo, & Lorenzini, 2016) and (Raju, Sandeep, & Malvandi, 2016). The non-uniform heat source model is a combination of temperature and space-dependent heat sources. (Sravanthi, 2019) studied nanoliquid flow over a rotating disk with the non-uniform heat source and recorded a negative

impact in the heat transfer rate with augmentation in space-dependent heat source parameters. (Song et al., 2022) noticed an enhanced temperature profile with increment in the space and temperature dependant heat generation parameters whereas entropy production is minimized due to the non-uniform heat source (see (Unyong, Vadivel, Govindaraju, Anbuvithya, & Gunasekaran, 2022)).

1.24.10 Carreau nanofluid

Carreau nanofluid model includes low and high shear rates which is an attracting aspect in non-Newtonian studies. It is used to represent many manufacturing and chemical engineering flows. (Eid, Mahny, Dar, & Muhammad, 2020) studied Carreau nanofluid flow on top of an expanding sheet and found out that power law index promotes velocity. The Carreau fluid flow on top of an elongating cylinder was numerically investigated by (I. Khan, Ullah, Malik, & Hussain, 2018). They noticed a reverse relationship in the drag force due to Weissenberg number. (Salahuddin, Hussain, Malik, Awais, & Khan, 2017) analysed the slip effects of Carreu nanofluid over an elongated cylinder and observed a high-velocity profile for dilatant fluid due to augmentation in Weissenberg number.
(Hayat, Ahmed, Alsaedi, & Abbasi, 2018) numerically studied the flow of Carreau-Yasuda nanofluid in the presence of mixed convection and hall current and observed an inverse effect for concentration profiles under thermophoresis and Brownian motion parameters. (M. Khan, Azam, & Alshomrani, 2017) investigated about the unsteady slip flow of Carreau nanofluid over a wedge. (M. M. Nandeppanavar, Kemparaju, & Shilpa, 2019) scrutinized the Carreau nanofluid flow over an exponentially stretching sheet in a saturated porous medium using fourth order Runge-Kutta shooting method. (M. Khan, Hussain, Malik, Salahuddin, & Aly, 2019) numerically analysed the Carreau fluid flow for generalized Fourier's and Fick's laws. They observed that the horizontal velocity enhances with an increase in wall thickness parameter, power-law index, Weissenberg number, thermal Grashof parameter and bioconvection Rayleigh number.

1.24.11 Reiner-Rivlin fluid

Non-Newtonian fluids are classified as shear thinning, shear thickening, rheopectic, and thixotropic. Many viscoelastic non-Newtonian fluids like power-law fluids, Ellis fluids, Prandtl fluids, and Reiner-Rivlin fluids have fascinated researchers

owing to their applicability. Non-Newtonian fluids possess an elastic and viscous nature. Reiner-Rivlin nanoliquid is a non-Newtonian fluid that exhibits the dilatancy phenomenon. Dilatancy is the ability associated with the volume of a material. Dilatant material acquires a higher volume by stirring. Some important non-Newtonian fluids such as food products, biological fluids, and polymers, can be effectively analyzed by Reiner-Rivlin's nanofluid model (see (Lv, Gul, Ramzan, Chung, & Bilal, 2021), (Rashid & Mustafa, 2021) and (Rafiq, Mustafa, & Khan, 2022)). (Tabassum & Mustafa, 2018) investigated the Reiner-Rivlin slip flow on a rotating rough disk. They observed that the skin friction and resisting torque were increased with an increment in parameters of wall roughness. (A. Das & Sahoo, 2018) analyzed heat transfer between rotating coaxial disks by using Reiner-Rivlin fluid. (Sahoo & Shevchuk, 2019) investigated the rotating Reiner-Rivlin fluid flow on a stretching surface. They concluded that a significant decrease in the thermal boundary layer occurred due to increased radial stretching. (Naqvi, Kim, Muhammad, Mallawi, & Ullah, 2020) examined the Reiner-Rivlin liquid flow on a spinning disk including slip conditions. They observed that a higher torque was required to preserve consistent disk rotation with high wall slip. (Abdal et al., 2021) implemented bioconvection on Reiner-Rivlin nanoliquid flow past a rotating disk and they reported that intensified values of Reiner-Rivlin fluid parameter decremented both the radial and azimuthal wall stress. (Sadiq & Hayat, 2022) addressed the Reiner-Rivlin nanoliquid flow due to an elongated rotating disk. The researchers constructed a convergent solution using the ND-solve method and observed an improvement in tangential velocity with an increase in Reiner-Rivlin fluid parameter.

1.24.12 Quadratic/non linear convection

Nonlinear thermal convection play a significant role in solar collectors, the manufacturing of electronic equipment, and the process of doping. In these situations, a linear approximation of the density variation with temperature may incur significant errors. (Vajravelu & Sastri, 1977) introduced nonlinear thermal convection which drew the attention of many researchers as seen in ((Mahanthesh & Mackolil, 2021), (Elshehabey, Raizah, Öztop, & Ahmed, 2020) and (Basha, Sivaraj, Prasad, & Beg, 2021)). (Raju, Saleem, Al-Qarni, & Upadhya, 2019) studied the nonlinear

convective fluid flow past a stretching sheet utilizing Eyring–Powell fluid model with the suspension of dust and graphene particles. The researchers found an inverse relationship between the Nusselt number and the nonlinear convection parameter. (Jha & Sarki, 2020) investigated the nonlinear convection near a moving plate and studied the heat and mass transfer effects. An increased fluid velocity in the case of nonlinear convection was reported.

1.24.13 Nanoparticle aggregation

Nanoparticles tend to form clusters known as nanoparticle aggregates. Rapid and moderate aggregation occurs depending on the interparticle characteristics of the nanoparticles and the chemistry of the base fluid. Aggregated nanoparticles possess different properties when compared to independently dispersed particles. (Ganguly, Basu, & Sikdar, 2012) investigated the cluster of nanoparticles from an aqueous suspension of Al_2O_3 with a volume fraction of 0.005 and observed an agglomeration size varying in the range 100-500 nm. Nanoparticle aggregates of stable nanofluids can significantly alter the heat transfer capacity of the working fluids (see (Wensel et al., 2008) and (Parameshwaran & Kalaiselvam, 2013)). The aggregation structure is described by the fractal dimensions which quantitatively measures the degree of openness or compactness of the aggregate structure (W. Zhang, 2014). (B.-X. Wang, Zhou, & Peng, 2003) described a fractal model and successfully predicted the thermal conductivity for low volume fractions of metallic oxide nanoparticles in the base fluid. (Chen, Ding, He, & Tan, 2007) effectively estimated the nanofluid thermal conductivity using aggregation of titanium dioxide (TiO_2) in EG base fluid. TiO_2 nanoparticles are widely used in cosmetics, toothpastes, plastics, paints and solar collectors and their aggregation characteristics have been discussed by researchers as seen in (Zhu, Wang, Keller, Wang, & Li, 2014), (Hu et al., 2018) and (V. K. Sharma, 2009). (Sindhu & Gireesha, 2020) studied the kinematics of nanofluid flow with nanoparticle aggregation through a microchannel. The researchers observed a high-temperature profile for the aggregation model when compared to the conventional models. (Mackolil & Mahanthesh, 2021b) analyzed the nanoparticle aggregation factor in the Marangoni convective flow of a nanofluid and scrutinized the sensitivity of the heat transfer rate. It is noticed that a lowered velocity profile due to aggregation effects.

1.24.14 Porous medium

Porous material includes voids and is characterized by porosity parameters. Studies relating to petroleum engineering, filtration, soil mechanics, and biological tissues utilize the idea of porous media. (Jafar, Shafie, & Ullah, 2020) analyzed nanofluid flow in a porous medium and they investigated an enhanced temperature profile with high porous parameter values. (Eid & Nafe, 2022) found a retarded velocity profile with incremented porous parameter values. Additionally, studies involving porous medium are discussed in (Krishna, Ahamad, & Chamkha, 2020) and (Z. Khan, Makinde, Hamid, Haq, & Khan, 2020).

1.24.15 Injection/suction

A permeable medium allows fluid penetration in the presence of more connected voids. The injection and suction effects due to the influence of permeability have a potential application in astronomical disciplines, fuel injection thermal protection and aerodynamics (see (Ganapathirao, Chamkha, & Srinivasa Rao, 2019), and (S. Rana, Mehmood, & Bhatti, 2021)). (Acharya, Maity, & Kundu, 2020) observed an amplified temperature profile in the presence of injection. (Nadeem, Abbas, & Malik, 2020) noticed an elevated boundary layer thickness in the presence of injection effects and the trend reversed with suction.

1.24.16 Convective boundary condition

Convective boundary condition creates a significant relation between thermal difference and heat flux at the surface (Zhao, Li, Wang, & Wang, 2022). (Sreedevi, Reddy, & Chamkha, 2018) found an enhanced heat transfer effect and (Saif, Muhammad, Sadia, & Ellahi, 2020) noticed an increment in the thermal boundary layer with elevation in the Biot number. (Patel & Singh, 2019) studied micropolar fluid flow over a stretched sheet with convective boundary conditions in the presence of Brownian motion and thermophoresis effects. An improvement in heat transfer due to increased Biot numbers was observed. (Ray, Vasu, Murthy, & Gorla, 2020) studied the non-similar solution of Eyring-Powell fluid flow and heat transfer with convective boundary conditions using HAM.

1.24.17 Radiation

(S. Das et al., 2016) reviewed the transient free convection nanofluid flow through a vertical channel in the presence of thermal radiation. MHD flow past a cosinusoidally fluctuating heated plate with radiation was researched by (Ram, Singh, Kumar, Kumar, & Joshi, 2017). (Nayak, Shaw, Pandey, & Chamkha, 2018) studied the combined effects of slip and convective boundary conditions on MHD three-dimensional stretched flow of nanofluid through porous media under nonlinear thermal radiation. (Kumar, Sood, Shehzad, & Sheikholeslami, 2017) investigated the non -Newtonian fluid flow past a Riga plate and the researchers found an elevation in the heat transfer rate with an increase in radiation parameter. (Mohammadein & El-Amin, 2000) investigated the influence of radiation on power-law fluid flow past a plate in a porous medium and the researchers noticed an increased temperature profile with radiation. Nanofluid flow with radiation effects are studied in (K. Das, Duari, & Kundu, 2014), (Hossain & Takhar, 1996) and (Sekhar et al., 2017)

1.24.18 Chemical reaction

(Haile & Shankar, 2014) examined the MHD nanofluid flow with heat and mass transfer through a porous medium with thermal radiation, viscous dissipation, and chemical reaction effects. The study showed that the effect of heat and mass transfer with chemical reaction has a significant role in processes like the transfer of energy in a wet cooling tower, drying, the flow in desert coolers, and electric power generation. Chemical reaction effect has a major role in industrial processes like the fabrication of ceramics or glassware and the production of polymers (Haile & Shankar, 2014). Nanofluid flow with chemical reaction can be found in (Kameswaran, Narayana, Sibanda, & Murthy, 2012), (Tarakaramu & Narayan, 2017), (C. Zhang, Zheng, Zhang, & Chen, 2015) and (Kumar, Sood, Sheikholeslami, & Shehzad, 2017).

1.24.19 Hall current

Hall current is developed in the flow of a conducting fluid normal to the strong magnetic field. (Hall et al., 1879) introduced the concept in 1879. Hall current has attracted many researchers due to its application in Hall accelerators, Hall sensors, magnetic resonance imaging, etc. (Lv, Shaheen, et al., 2021). An oscillatory MHD flow through a rotating channel in the presence of a Hall current has been analyzed previously by (Pal & Talukdar, 2013). (Tlili, Ramzan, Kadry, Kim, &

Nam, 2020) analyzed Hall effect on hydromagnetic flow past a moving thin needle and the researchers noticed an enhanced velocity profile with an increase in the Hall parameter.

1.24.20 Soret effect

Whenever there are different chemical species present under a strong temperature gradient, the Soret effect is significant. (Hayat, Aslam, Khan, Khan, & Alsaedi, 2019) studied the Soret effect on peristalsis flow through an inclined channel utilizing pseudoplastic fluid and the researchers addressed a declined concentration profile with an increase in Soret number. Hydromagnetic flow with Soret effect can be found in the studies of (S. A. Khan, Hayat, Khan, & Alsaedi, 2020), (S. A. Khan et al., 2020), (Krishna et al., 2019) and (Hayat, Shehzad, & Alsaedi, 2012).

1.24.21 Joule heating

The Joule heating process can be seen in food processing equipment, soldering irons, electric kettles, and electric stoves. On the other hand, excess heat during the procedure is harmful to numerous systems. Therefore Joule heating is crucial. (Gayatri, Jayarami Reddy, & Jayachandra Babu, 2020) studied the influence of Joule heating on a two-dimensional Carreau fluid flow past a stretching sheet. (Kempannagari, Buruju, Naramgari, & Vangala, 2020) discussed Joule heating effect on hydromagnetic non-Newtonian flow past a curved surface. Hydromagnetic flow with joule heating effect is discussed in (Gireesha et al., 2019), (Iqbal, Khan, Ahmed, & Nadeem, 2020) and (Wakif et al., 2020).

1.24.22 Various models depicting nanofluid flow

Buongiorno presented a model in 2006 based on seven slip mechanisms such as gravity, Magnus effect, fluid drainage, thermophoresis, diffusiophoresis, Brownian random motion, and inertia. Among them, thermophoresis and Brownian diffusion were found to be the most imperative. (Kho, Hussanan, Mohamed, & Salleh, 2019) utilized the Buongiorno model to analyze the heat transfer properties of the Williamson nanofluid considering thermophoresis and Brownian motion. They reported enhanced concentration and temperature profiles with the increment in the Williamson parameter. (S. E. Ahmed & Rashed, 2019) explained the thermophoretic and random motion effects in a wavy porous enclosure. (Sheikholeslami, Chamkha, Rana, & Moradi, 2017) scrutinized the impact of nanoparticles via Brownian random

motion and thermophoretic effect in the free convection through an enclosure of L-shape. They incorporated the CVFEM method for the computations. Rotating disk fluid transport of an Oldroyd-B nanofluid was explored by (Hafeez, Khan, & Ahmed, 2020). A drop in the heat transfer rate was observed in their study with the variations in Brownian random motion and thermophoretic parameters. Nanofluid flow over various attributes utilizing Buongiorno model can be found in (De, 2019b), (S. Reddy, Bala Anki Reddy, & Rashad, 2020), (De, 2019a), (Roşca, Roşca, Pop, & Merkin, 2020) and (De & Gorji, 2020). (Zeeshan, Maskeen, & Mehmood, 2018) presented MHD flow over a stretched cylinder using Buongiorno's model and observed that the concentration profile declined due to Brownian motion.

However, the Buongiorno model excludes the augmentation in the effective thermophysical properties of nanomaterial. In 2003, (Khanafer, Vafai, & Lightstone, 2003) developed a nanoliquid transport model considering the nanoparticle dispersion. Later, (Tiwari & Das, 2007) developed a simpler nanofluid model considering the effective thermophysical properties of a nanofluid. (Kumar, Kumar, Shehzad, & Sheikholeslami, 2018) utilized the Tiwari-Das nanofluid model to investigate the influence of vibrational rotations and multiple slip conditions on the hydromagnetic nanomaterial flow over an elongating surface. They observed a rise in the Nusselt number for augmenting nanoparticle volume fraction.

Modified Buongiorno nanoliquid model (MBNM) extends the traditional Buongiorno model by considering the effectual slip mechanisms along with the effective properties of a nanofluid. (Yang, Li, & Nakayama, 2013) modified the Buongiorno model for the impact of volume fraction of nanoparticles in the equations describing the fluid flow. The heat transfer of a nanoliquid over an elongated sheet involving MBNM was studied by (P. Rana, Shukla, Bég, & Bhardwaj, 2021). (Mahanthesh, Shashikumar, & Lorenzini, 2021) utilized MBNM to model the nanoliquid flow over a wedge. Higher sensitivity towards the heat transfer rate was exhibited by the Brownian motion parameter. Further discussions on the flow problems modelled using MBNM can be seen in (Ray, Vasu, Bég, Gorla, & Murthy, 2019), (Wakif, Chamkha, Thumma, Animasaun, & Sehaqui, 2021), (Mahanthesh & Mackolil, 2021), (Areekara, Mackolil, Mahanthesh, Mathew, & Rana, 2022) and (P. Rana, Srikantha, Muhammad, & Gupta, 2021).

1.24.23 Nanofluid flow with slip effects

At microscopic interfaces, the velocity of the fluid (near the wall) may not be always considered zero due to the occurrence of a relative movement between the wall and the fluid. In these situations, the velocity of the fluid at the interface is assumed to be a constant multiple of wall shear stress and this constant multiple (measured in length) that extrapolates velocity is named the velocity slip parameter (or hydrodynamic slip parameter). Slip flow plays a significant role in engineering and medical field. Micro valves, hard disk drives, internal cavities and nozzles are a few examples where the slip flow is utilized. (Ramya, Raju, Rao, & Chamkha, 2018) investigated a decreased velocity profile with augmented values of velocity slip. The significance of hydrodynamic slip and viscous dissipation over a stretching/shrinking surface was studied by (Aly & Pop, 2020). A comparative analysis between the hybrid and traditional nanofluid on the effect of slip parameter showcased the superior cooling capability of the hybrid nanoliquid. Further studies exploring velocity slip effects are discussed in (S. U. Khan, Waqas, Muhammad, Imran, & Aly, 2020), (M. I. Khan, Alzahrani, Hobiny, & Ali, 2020) and (I. C. Mandal, Mukhopadhyay, & Vajravelu, 2021). (Vinita & Poply, 2020) studied slip flow past a stretched cylinder and found a reduced velocity profile due to the slip parameter. Non-Newtonian and Newtonian fluids with slip effects are reviewed by numerous researchers. Effect of thermal slip and velocity slip past a stretching cylinder are found in (Ogunseye, Sibanda, & Mondal, 2019), (Mishra & Kumar, 2020) and (Usman, Soomro, Haq, Wang, & Defterli, 2018). (Sadiq, Haider, Hayat, & Alsaedi, 2020) illustrated the effects of thermal slip in Darcy-Forchheimer nanofluid flow by a rotating disk. They observed that the heat transfer rate is an increasing function of the thermal slip parameter. In addition, (Ramzan et al., 2021) noticed a decline in the thermal boundary layer due to the increasing thermal slip parameter. Thermo-hydrodynamic (thermal and velocity) slip plays a major role in the applications like polishing of surfaces, micro devices, and mechanical heart valves (see (Mishra & Kumar, 2020)).

1.24.24 Zero mass flux condition/Passive control approach

(Kuznetsov & Nield, 2013) introduced a physically more realistic model which involves the passive control of the nanoparticle volume fraction at the boundary. Nanofluid flow past a stretching sheet with zero mass flux condition is discussed in

(Sudarsana Reddy & Sreedevi, 2021) and (Faisal, Ahmad, & Javed, 2021). Mass flux corresponds to the rate of mass flow per unit area perpendicular to the direction of flow. Zero mass flux is the condition when the normal flux of nanoparticles is zero at the boundary. (Ramzan, Sheikholeslami, Saeed, & Chung, 2019) examined the flow of couple stress nanofluid past an exponential stretched surface and observed that for growing values of Brownian motion and thermophoresis parameters, the concentration profile exhibits decreasing and increasing behaviour respectively. (Uddin et al., 2018) investigated the characteristics of buoyancy forces on stagnation point flow under magneto-nanoparticles and zero mass flux condition. Characteristics of a thermally stratified flow of Sutterby nanofluid along with zero mass flux condition was analysed by (Mir et al., 2020).

1.24.25 Darcy-Forchheimer flow

Darcy's law corresponds to an equation that explains the capability of a fluid to flow via a porous medium. Darcy-Forchheimer flow is a fluid flow through a porous medium satisfying the Darcy-Forchheimer relation that subsumes inertial properties and boundary characteristics. The Darcy-Forchheimer nanoliquid flow due to a curved lengthening sheet has been numerically examined by (Hayat, Qayyum, Alsaedi, & Ahmad, 2020). They noted a decline in the velocity profile for mounting values of the Forchheimer number. (Alzahrani, Ullah, Alshomrani, & Gul, 2021) elucidated the significance of Darcy-Forchheimer hybrid nanoliquid flow over an inclined solar collector plate. Studies discussing the three-dimensional Darcy-Forchheimer flow over a lengthening sheet can be seen in (Kumar, Sharma, Kumar, Sheikholeslami, & Vajravelu, 2021), (Ullah, Muhammad, & Mallawi, 2021), (Jawad, Saeed, Khan, & Islam, 2021), (Shankaralingappa, Gireesha, Prasannakumara, & Nagaraja, 2021), (Xiong, Chu, Khan, Khan, & Abbas, 2021) and (Joshi, Upreti, & Pandey, 2022).

1.24.26 Nanofluids with various shapes of nanoparticles

Nanofluids with various nanoparticle shape exhibits differing thermal and physical properties. In 2009, (Timofeeva et al., 2009) discussed the consequence of different shaped alumina nanoparticles (platelet, blade, brick, and cylinder) on its thermo-physical properties and predicted a model for effective thermal conductivity and effective dynamic viscosity based on the experimental data. In addition, (Kim, Lee, Lee, & Jang, 2015) experimentally concluded that the liquid suspension with

brick-shaped alumina nanoparticles showcased the highest thermal conductivity. Recently, the fluid characteristics and heat transfer capabilities of nanofluid flow through a horizontal tube with various nanoparticle shapes were investigated by (Benkhedda, Boufendi, Tayebi, & Chamkha, 2020) and observed higher heat rates for the platelet-shaped nanoparticles. In addition, (Bahiraei, Monavari, & Moayedi, 2020) noticed that the maximum frictional entropy generation belonged to the platelet-shaped nanoparticles and the minimum frictional entropy generation belonged to the Os-shaped nanoparticles.
(Mahanthesh, Gireesha, Shehzad, Rauf, & Kumar, 2018) explored the effects of various nanoparticles of column, lamina, sphere, hexahedron, and tetrahedron-shaped nanoparticles in a magnetohydrodynamic flow due to a rotating disk and detected an increased nanofluid temperature for sphere-shaped nanoparticles. (Saranya & Al-Mdallal, 2021) examined the effect of nanoparticle shapes (sphere, cylinder, brick, blade, and platelet) on the alumina-silicon oil nanofluid flow due to a rotating disk. They observed that the blade-shaped nanoparticles displayed the highest thermal conductivity followed by platelet, cylinder, brick, and sphere-shaped nanoparticles. Further, (Waqas, Farooq, Naseem, Hussain, & Alghamdi, 2021) analyzed the impact of the sphere, platelet, and cylindrical-shaped nanoparticles on the hybrid nanofluid flow due to a rotating disk.

1.25 Objectives

The main objectives of the present work are to investigate

- Various mathematical models describing hydromagnetic flows
- Numerical methods to solve MHD convective nanofluids
- The effectiveness of heat transfer enhancement in different nano fluids with different parameters
- The applicability of nanofluids in optimizing drag coefficient
- The comparison of theoretical findings with statistical results